

---

## Genomic abnormalities affecting mussels (*Mytilus edulis-galloprovincialis*) in France are related to ongoing neoplastic processes, evidenced by dual flow cytometry and cell monolayer analyses

Benabdelmouna Abdellah<sup>1,\*</sup>, Saunier Alice<sup>1</sup>, Ledu Christophe<sup>1</sup>, Travers Marie-Agnes<sup>1</sup>, Morga Benjamin<sup>1</sup>

<sup>1</sup> IFREMER, PDG-RBE-SGMM-LGPMM, Station de La Tremblade, Avenue de Mus de Loup, F-17390 La Tremblade, France

\* Corresponding author : Abdellah Benabdelmouna, email address : [Abdellah.Benabdelmouna@ifremer.fr](mailto:Abdellah.Benabdelmouna@ifremer.fr)

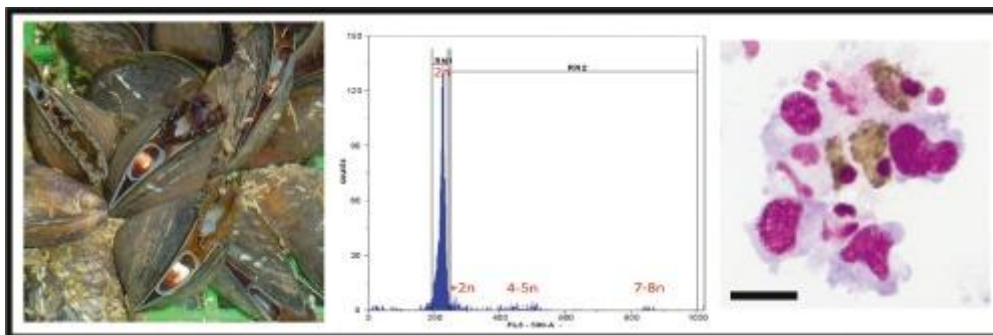
---

### Abstract :

In the context of the abnormal mass mortality of mussels in France since 2014, Flow CytoMetry (FCM) was used in 2015 and 2016 to study the DNA content and cell cycle characteristics of hemic circulating cells collected from 2000 mussels. The mussels were sampled from 12 wild and cultivated blue mussels stocks distributed along the French Atlantic coast from the south Brittany to Pertuis Charentais areas. During these surveys, various genetic abnormalities were frequently detected, and ploidy characteristics revealed contrasting profiles that corresponded to respective contrasting sanitary status, i.e. healthy mussels with high cytogenetic quality (HCQ) *versus* diseased mussels with low cytogenetic quality (LCQ). In the present work, FCM and hemocytology cell monolayer techniques were combined in order to determine the putative causes of the observed genetic abnormalities that were significantly associated with mortality levels. FCM and cell monolayer approaches permitted the definition of new threshold values delimiting HCQ mussels from LCQ ones. FCM histograms of mussels from the HCQ group showed one single or a largely dominant population of diploid (2n) nuclei and a large majority of normal hemocytes. Hemolymph cell-monolayer analyses showed predominantly acidophil granulocytes characterized by nuclei of normal size and a large cytoplasm with numerous granulations. In contrast, FCM histograms for the LCQ group showed, in addition to the normal diploid (2n) nuclei, populations of nuclei that displayed aneuploidy patterns in a broad ploidy range, including diploid-triploid (2–3n), tetraploid-pentaploid (4–5n) and heptaploid-octaploid levels (7–8n). The corresponding hemolymph cell-monolayer showed cellular features characteristic of disseminated neoplasia disease with frequent abnormal anaplastic cells that exhibited noticeable numbers of mitotic figures with both normal and aberrant chromosomes segregation patterns. These neoplastic cells were a rounded shape with a reduced, granulation-free cytoplasm and large (11–12 µm) to very large (up to 21 µm) round or ovoid nuclei that correspond to the 4–5n and 7–8n nuclei previously detected by FCM analyses. These characteristics suggest that the genetic abnormalities detected by means of FCM were related to an ongoing neoplastic process that is affecting blue mussels in France, at least since the onset in 2014 of

the mortality that heavily impacted French blue mussels stocks

### Graphical abstract



### Highlights

- ▶ Percentages of non-diploid nuclei in mussel hemolymph could vary from 2% to 25%.
- ▶ FCM analysis constituted two contrasted groups that were further characterized by cell monolayer approach.
- ▶ New threshold values to qualify the cytogenetic quality of mussels were established.
- ▶ Hemocytes of animals with low cytogenetic quality presented enlarged nuclei and mitotic figures.
- ▶ We propose that the genomic abnormalities are related to ongoing neoplastic process.

**Keywords :** Mussels, Hemocytes, Flow cytometry, Hemocytology, Cytogenetic quality, Neoplasia

61           **1. Introduction**

62           In France, farming of *Mytilus* spp. consisting of the blue mussel *Mytilus edulis*, the  
63 Mediterranean mussel *M. galloprovincialis* and hybrids of both species is an important  
64 industry with production varying during the last decade from 71,000 to 79,000 metric tons per  
65 year (FAO, 2014). However, the production of French mussels has decreased dramatically  
66 since 2014 because of sudden and unfamiliar mass mortality (90-100%) of both juvenile and  
67 adult mussels cultivated at various French Atlantic areas, including south and north Brittany,  
68 Bourgneuf Bay and Charentais Sound (Béchemin et al., 2015). Mortality of both naturally  
69 occurring and cultured blue mussels has been reported in many other locations around the  
70 world (Tremblay et al., 1998; Myrand et al., 2000; Fuentes et al., 2002). The extent of  
71 mortality can be highly variable and several stress-related factors have been investigated,  
72 including pathogens, pollution, temperature, food depletion and reproduction, leading to a  
73 preliminary conclusion that none of these factors alone can explain the cause. Although blue  
74 mussels are generally considered to be resilient to environmental disturbances and pollutants;  
75 several studies have shown that the exposure of mussels to environmental contaminants  
76 results in DNA damage. Damage includes abnormalities in DNA content and structure, as  
77 well as the progressive development of circulating aneuploid-polyploid cells in the  
78 hemolymph, in particular the development of a fatal leukemia-like cancer disease called  
79 hemic (or disseminated) neoplasia (Elston et al., 1992; Bihari et al., 2003; Vassilenko and  
80 Baldwin 2014). This malignant disease has been reported in 15 species of marine bivalves  
81 with a world-wide distribution that includes the cockle *Cerastoderma edule*, four species of  
82 oysters, six species of clams and five species of mussels (Farley et al., 1986; Elston et al.,  
83 1992; Villalba et al., 1995; Villalba et al., 2001; da Silva et al., 2005; Delaporte et al., 2008;  
84 Galimany and Sunila 2008; Le Grand et al., 2010; Diaz et al., 2011). The disease is  
85 characterized by proliferation of anaplastic circulating cells with enlarged and pleiomorphic

86 nuclei, a high nucleus-to-cytoplasm ratio and frequent presence of mitotic figures (Elston et  
87 al., 1992). In late stages, anaplastic cells completely replace normal hemocytes and penetrate  
88 various tissues such as connective tissue, gonads, the mantle and foot (Barber 2004; Carballal  
89 et al., 2015). This disease is progressive and commonly fatal causing significant mortality and  
90 decrease in market harvests of economically important species (Bower 1989; Elston et al.,  
91 1992; Barber 2004, Carballal et al., 2015).

92 In the context of the abnormal outbreaks of mass mortality of blue mussels in France  
93 since 2014, it was hypothesized that mortality was probably linked to poor cytogenetic  
94 quality, particularly in terms of ploidy variations and cell cycle DNA alterations affecting  
95 circulating cells in the hemolymph. These genetic abnormalities can be reliably studied by  
96 Flow CytoMetry (FCM) methods (Elston et al., 1990; Moore et al., 1991; Reno et al., 1994;  
97 Da Silva et al., 2005, Vassilenko and Baldwin 2014). FCM was used in a previous study to  
98 investigate the DNA content and cell cycle characteristics of hemic cells collected from  
99 various wild and cultivated mussels stocks that had, at our best knowledge, no history of  
100 mortality before 2014 and that showed much higher mortality levels after that time  
101 (Benabdelmouna and Ledu 2016). In that survey, different thresholds of genetic abnormality  
102 (GA%) were established and appeared to be highly predictive of the final mortality levels.  
103 Interestingly, ploidy characteristics of hemic cells revealed contrasting profiles, which  
104 corresponded to respective contrasting sanitary status, apparently healthy *vs* diseased mussels.  
105 Normal healthy mussels were shown to be of high cytogenetic quality (HCQ) and contained  
106 nearly entirely diploid cells in their hemolymph while abnormal diseased mussels had low  
107 cytogenetic quality (LCQ) and contained, in addition to normal diploid cells, a broad  
108 continuum of aneuploid-polyploid cells that could either be linked to genotoxic effects of  
109 unknown origin and/or most probably to ongoing hemic neoplasia disease.

110 From the Benabdelmouna and Ledu (2016) study, it was apparent that systematically  
111 combining FCM and light microscopy methods (especially hemocytology by cell monolayer  
112 technique) would be beneficial in order to *i)* determine the putative cause of the observed  
113 genetic abnormalities, *ii)* to characterize at the cellular level the disorder during mussel  
114 mortality events, and *iii)* determine more precise thresholds of genomic abnormality (GA%)  
115 that could provide tools to manage mortality outbreaks. For this purpose, non-invasive FCM  
116 analyses were used to preliminarily constitute two groups of blue mussels of cytogenetic  
117 quality LCQ and HCQ. Individual mussels were then subjected to hemocytology exams by  
118 the cell monolayer technique (“cytospin®”) in order to establish a clear relationship between  
119 FCM-based cytogenetic quality status and the corresponding cellular and cytological  
120 characteristics of hemocytes.

121

122 **Material and Methods**

123 **Biological material**

124 Adult mussels used in this study were randomly collected during April 2017 from a  
125 wooden pole “bouchot” grow-out facility dedicated to mussel culture and located along the  
126 English Channel at Donville les Bains in western Normandy, France (48°52’957N;  
127 00°34’892W). Farmer’s mussel seed were originally collected during spring 2016 from  
128 natural spatfall at Fouras in the Pertuis Charentais area of the Atlantic coast. At the end of  
129 Summer 2016, mussel spat of less than 1 mm shell length that settled on coconut fiber ropes  
130 at a mean density of 10,000 individuals per meter were transferred to their final growing zone  
131 at Donville les Bains. In April 2017, following a brief mortality event of about 15%, 300 live  
132 adult mussels of 3 - 6 cm shell length were transported to our LGPMM experimental hatchery  
133 at LaTremblade where they were maintained in a separate tank alimented through 250-L per  
134 hour of unheated and UV-filtered seawater

135

136 **Hemolymph collection**

137 Mussels were anaesthetized in a solution containing 50 g L<sup>-1</sup> of magnesium chloride  
138 until the valves opened. Hemolymph was withdrawn in a non-destructive manner from the  
139 adductor muscle of each individual mussel with sterile 1 mL syringe fitted with a 26 gauge  
140 needle. For each animal, a volume of approximately 0.2 mL of hemolymph was collected and  
141 stored for less than 5 min in an Eppendorf microcentrifuge tube on ice to prevent clumping.  
142 Each hemolymph sample was immediately subjected to FCM and cell monolayer analyses.

143

144 **Flow cytometry analysis**

145 FCM analyses were conducted as described in Benabdelmouna and Ledu (2016). In  
146 brief, 0.1 mL of hemolymph collected from each individual mussel was used for nuclei  
147 extraction and staining. The samples were first collected in a 1.5 mL Eppendorf tube  
148 containing 1 mL of nuclei extraction buffer (5 mM MgCl<sub>2</sub>, 85 mM NaCl, 10 mM Tris, 0.1%  
149 Triton X-100, pH 7) and the nuclei were then collected by filtration through a 30- $\mu$ m nylon  
150 sieve. Samples were simultaneously treated with DNase-free RNase A (50  $\mu$ g mL<sup>-1</sup>, Sigma,  
151 R4875, Saint-Louis, MI, US) and stained at room temperature for 30 min in the dark with  
152 propidium iodide (PI, Sigma, P4170, Saint-Louis, MI, US) at a concentration of 50  $\mu$ g mL<sup>-1</sup>  
153 in a 2-mL final solution. FCM was performed on a Partec PA II flow cytometer equipped with  
154 a 590 nm, 30 mW green laser (Sysmex, Sainte Geneviève des Bois, France). Peak position  
155 and cell-cycle estimates were done as described in Benabdelmouna and Ledu (2016). In order  
156 to distinguish nuclei in the G<sub>2</sub>/M phase from doublets of G<sub>0</sub>/G<sub>1</sub> nuclei that have the same  
157 DNA content, FL3-area vs FL3-width dot-plots were used to gate single nuclei. Thus a region  
158 (R1) was drawn on these dot-plot representations to discriminate single nuclei from doublets.  
159 After gating them on R1, single nuclei were next plotted on a FL3-area histogram on 1024  
160 linear scale and used to calculate the percentages of nuclei populations according to their  
161 DNA content. Selection of the two mussel groups according to their cytogenetic quality status  
162 (LCQ vs HCQ) was done according to our previous work (Benabdelmouna and Ledu 2016)  
163 that fixed an upper limit of 10% of non-diploid nuclei for a normal HCQ mussel. Beyond this  
164 limit, mussels were considered abnormal with a LCQ status.

165

### 166 **Cell monolayer analysis**

167 Hemocytological analyses by cell monolayer technique were conducted for individuals  
168 with contrasting FCM profiles constituting the LCQ and HCQ groups. For each of these

169 selected mussels, 40  $\mu$ L of freshly collected hemolymph taken from the venous sinuses in the  
170 adductor muscle were pipette onto a poly-L-lysine coated glass slides for cyto-centrifugation  
171 (4°C, 1 min, 500 rpm – Universal 16R, Hettich-Zentrifugen, Tuttlingen, Germany).  
172 Supernatant was removed; each slide was dried at room temperature and then stained with  
173 hematoxylin-eosin and observed under light microscopy (BX50, Olympus, Tokyo, Japan).  
174 Digital images were also captured using a Zeiss Axioplan 2 Imaging microscope, and  
175 digitized images were prepared for printing in Axiovision software (Zeiss).

176           Twenty individuals were analyzed; ten each of HCQ and LCQ condition. A total of  
177 150 cells was counted per sample for three cell types (granulocytes, normal hyalinocytes and  
178 mitotic figures) and measured using Stream Essential software (v.1.9.3).

179

## 180 **Statistical analysis**

181           Based on the ploidy level variation, two cytogenetic qualities were defined: HCQ  
182 (n=10 specimens, n=150 cell/specimen) and LCQ (n=10 specimens, n=150 cell/specimen).  
183 Normality of the residuals using the Shapiro test, homoscedasticity using the Bartlett test and  
184 then non parametric Wilcoxon test were performed to compare these two groups using R  
185 software (v.1.0.153, RStudio Team, 2015). Plots were performed using *ggplot2* package  
186 (Wickham, 2009).

187

188 **Results**

189           During the week of their reception in the hatchery, 128 mussels of 5 cm mean shell  
190 length randomly collected from “Donville les Bains” were individually analyzed by FCM in  
191 order to contrast the two groups, HCQ *versus* LCQ. FCM analyses permitted the calculation  
192 of the respective percentages of non-diploid nuclei ( $\%>2n$ ) in the hemolymph from each  
193 mussel and the qualification of its cytogenetic status (LCQ *versus* HCQ). FCM analyses of  
194 mussels from this site showed that the percentages of non-diploid nuclei in the hemolymph  
195 varied from 2% to 25%, with a mean value of genetic abnormality (GA%) of 10% for this  
196 site. Of the 128 analyzed mussels, 68 (53.1%) were determined to have an LCQ status while  
197 the remaining mussels (46.9%) were of HCQ status. Sixty mussels were then selected to  
198 contrast the two groups. The LCQ group contained 40 mussels with the highest percentages of  
199 non-diploid nuclei, varying from 10% to 25% (average 19.9%), while the HCQ group  
200 contained 20 mussels with the lowest percentages of non-diploid nuclei, varying from 2 to  
201 5.6% (average 3.1%), a statistically significant difference ( $p < 0.001$ ; Wilcoxon test) (**Fig. 1**).

202           To establish a clear relationship between the FCM-based cytogenetic quality status  
203 and the correspondent cellular and cytological characteristics of hemocytes collected from  
204 individual mussels in the LCQ and HCQ groups, we compared the FCM patterns and their  
205 corresponding cytological figures obtained in the cell monolayer approach. FCM histograms  
206 of mussels from the HCQ group showed one single or very largely dominant population of  
207 diploid ( $2n$ ) nuclei in the G0/G1 phase (**Fig. 2a**). Hemolymph cell-monolayers from the HCQ  
208 mussels, and more especially those that exhibited less than 5% of non-diploid nuclei in their  
209 hemolymph (**Fig. 2b**), showed a large majority of normal hemocytes with nucleus stained  
210 dark purple and cytoplasm light purple. Typical hemocytes of HCQ mussels were  
211 predominantly acidophile granulocytes with high cytoplasm to nucleus ratio and were  
212 characterized by nuclei of normal size (mean size of  $5.7 \pm 1.2 \mu\text{m}$ ) and large cytoplasm with

213 numerous granulations. In addition, some basophile hyalinocytes with low cytoplasm/nucleus  
214 ratio were detected with a nucleus of normal size enclosed in a much reduced cytoplasm.

215         Mussels from the LCQ group presented FCM histograms with more complex patterns,  
216 showing, in addition to the normal diploid population of cells, additional populations of cells  
217 with non-diploid nuclei displaying aneuploidy patterns, a broad ploidy range including  
218 diploid-triploid (2-3n), tetraploid-pentaploid (4-5n, **Fig. 3A**) and even heptaploid-octaploid  
219 levels (7-8n, **Fig. 3B**). Abnormal cells were observed in the corresponding hemolymph cell-  
220 monolayer slides from LCQ mussels; proportions varied similarly to variation of ploidy  
221 levels, indicating most probably different disease status in the LCQ group. Compared to  
222 normal diploid cells with nuclei of normal mean size (5-6  $\mu\text{m}$  of diameter), the abnormal  
223 neoplastic cells were rounded with a reduced, granulation-free cytoplasm and large (11-12  
224  $\mu\text{m}$ ) to very large (up to 20  $\mu\text{m}$ ) round or ovoid nuclei that probably correspond to the 4-5n  
225 and 7-8n nuclei previously detected by FCM analyses (**Fig. 4**). Examination of cell monolayer  
226 patterns obtained from the different mussel groups showed the presence of frequent mitotic  
227 figures with both normal and aberrant chromosomes segregation patterns (**Fig. 4**).

228         Cell monolayer analyses of hemolymph samples from additional HCQ mussels with  
229 intermediate percentages of non-diploid nuclei (6 - 10%) also exhibited abnormal cells and  
230 mitotic figures but at a lesser extent than in LCQ mussels with < 10% non-diploid nuclei (not  
231 shown).

232         Based on cell characteristics (cell types, mean size of nuclei and percentage of mitotic  
233 figures), examination of ten individuals from each of the LCQ and HCQ mussel groups  
234 showed statistical differences for mitotic figures and normal hyalinocytes. While the number  
235 of mitotic figures was significantly higher in LCQ than in HCQ specimens (median: 27.2 vs  
236 6.3,  $p < 0.001$ , unilateral Wilcoxon test), the number of normal hyalinocytes was statistically

237 lower in LCQ than HCQ (median: 41.1 vs 72.9,  $p < 0.001$ , unilateral Wilcoxon test,). No  
238 difference was observed for number of granulocytes between LCQ and HCQ groups (**Fig.**  
239 **5A**). Finally, whereas the median size of nuclei was  $5.7 \pm 1.2 \mu\text{m}$  for HCQ specimens, nuclei  
240 of LCQ individuals were significantly larger at  $7.5 \pm 2.4 \mu\text{m}$  ( $p < 0.001$ , unilateral Wilcoxon  
241 test, **Fig. 5B**).

242

243 Discussion

244 Since 2014, the French *Mytilus* spp. industry has faced outbreaks of mortality rates of 90-  
245 100%, affecting both juveniles and adults. A previous study reported the presence of genetic  
246 abnormalities affecting hemic cells that also showed characteristics suggesting disseminated  
247 neoplasia disease (Benabdelmouna and Ledu, 2016). In that study, the extent of these genetic  
248 abnormalities was shown to be significantly correlated with mortality levels of blue mussels.

249 In the present work, flow cytometry analysis and cell monolayer analysis appeared to  
250 be efficient and complementary to detect abnormal neoplastic cells. These techniques allowed  
251 direct observation of a higher quantity of hemic cells, the primary host cell type affected by  
252 the disease. In addition, the cell monolayer technique avoids other cell types and histological  
253 structures that hamper observation of abnormal cells.

254 Hemocytology of LCQ mussels showed morphological characteristics that are  
255 consistent with disseminated neoplasia reported in other bivalve species (Barber 2004;  
256 Carballal et al., 2015). Specifically, similarities included anaplasia with affected cells  
257 presenting an undifferentiated aspect, and proliferative character with abundant mitotic  
258 figures present and frequent abnormal chromosomal segregation patterns. Simultaneous use of  
259 FCM and cell monolayer techniques showed 6-10% non-diploid nuclei in HCQ mussels, but  
260 with some abnormal cells in their hemolymph, suggesting that these mussels may be in  
261 transition to LCQ status. As a consequence, we believe that the threshold value of non-diploid  
262 nuclei in the hemolymph should be lowered to 5% to delimit HCQ mussels from LCQ  
263 mussels.

264 Previous FCM studies reported that mussel neoplastic cells were either 4n or 5n  
265 (Elston et al., 1990; Moore et al., 1991). In addition to the normal diploid nuclei and to the  
266 already described tetraploid-pentaploid (4-5n) neoplastic nuclei, we observed populations of

267 nuclei that displayed aneuploidy patterns including diploid-triploid (2-3n) and heptaploid-  
268 octaploid levels (7-8n). The corresponding hemolymph cell-monolayer figures showed  
269 cellular features that could be directly linked to the various ploidy levels described above.  
270 These neoplastic cells were of rounded shape with a reduced, granular-free cytoplasm and  
271 large (11-12  $\mu\text{m}$ ) to very large (up to 21  $\mu\text{m}$ ) round or ovoid nuclei. Assuming that a normal  
272 diploid nucleus has a mean size of 5.7  $\mu\text{m}$ , we concluded that 11-12  $\mu\text{m}$  nuclei and 21  $\mu\text{m}$   
273 nuclei correspond to the aneuploid 4-5n and 7-8n nuclei, respectively, previously detected by  
274 FCM analyses. It was apparent that this increase in DNA in circulating neoplastic cells  
275 occurred in parallel with the morphological changes described in hemocytological  
276 preparations. In bivalve molluscs with disseminated neoplasia, the alterations in ploidy appear  
277 to be closely related to alterations in nuclear structure. The fact that nuclear hypertrophy in  
278 bivalves results from the polyploidy of neoplastic cells was previously reported in various  
279 bivalve molluscs including *Mytilus* sp. (Moore et al., 1991; Carella et al., 2013, Vassilenko  
280 and Baldwin 2014; Carella et al., 2017), *Cerastoderma edule* (Collins, 1998; da Silva et al.,  
281 2005), *Limecola balthica* (Smolarz et al., 2005) and *Mya arenaria* (Reno et al., 1994;  
282 Delaporte et al., 2008). In these cases, the genetic abnormalities linked to neoplasia comprised  
283 various small to large-scale cytogenetic alterations, including principally aneuploidies and  
284 whole genome multiplications.

285         The neoplastic LCQ mussels analyzed exhibited the coexistence of several aneuploid  
286 peaks. This phenomenon has been observed in bivalve species affected by mortality  
287 outbreaks, including mussels (Elston et al., 1990; Moore et al., 1991) and cockles (Collins,  
288 1998; da Silva et al., 2005; Legrand et al., 2010), and was also found in studies where an  
289 increase in ploidy in the neoplastic cell populations is described during the progression of the  
290 disease (Elston et al., 1990; Legrand et al., 2010). Based on FCM, Elston et al. (1990)  
291 demonstrated that the progressive nature of the disease was evidenced by progressive

292 increases in abnormal polyploid cell populations and decreases in the proportion of normal  
293 diploid cells. The same authors suggested that cells in the non-diploid peak could correspond  
294 to neoplastic cells undergoing mitosis as the ratio between the second and first peaks is often  
295 close to 2.0. In cockles, Legrand et al., (2010) proposed two hypotheses to explain this  
296 pattern: (1) the presence of two concomitant neoplasia mechanisms developing within a single  
297 individual, each mechanism leading to a unique but different ploidy peak, or (2) an altered  
298 cell-division mechanism of neoplastic cells undergoing mitosis. Interestingly, in our present  
299 work, frequent abnormal mitotic forms were observed showing various abnormal  
300 chromosome segregation patterns. This finding supports the second explanation proposed  
301 above and we also suggest that abnormal mitosis is an important mechanism in the neoplastic  
302 processes affecting the blue mussels. In addition, histopathological examination of diseased  
303 mussels revealed many abnormal mitoses, and abnormal multipolar mitoses have been  
304 previously described in mussels from various geographical regions (Farley, 1969; Reno et al.,  
305 1994; Usheva and Frolova, 2000). As in vertebrates, frequency of abnormal mitoses seems to  
306 serve as a distinctive criterion for tumor progression in bivalve molluscs. It is noteworthy that  
307 in the present work, mitotic figures were found to be more frequent in LCQ mussels with low  
308 percentages of non-diploid nuclei than in LCQ mussels with high percentages of non-diploid  
309 nuclei. Sunila (1991) suggested that the level of mitotic activity of neoplastic cells in the  
310 hemolymph depended on the stage of neoplasm development. The highest mitotic index  
311 values were recorded at the early stages of the hemolymph neoplasia, when less than 10% of  
312 hemocytes in *M. arenaria* are replaced by the neoplastic cells. At the terminal stages, the  
313 mitotic index of *M. arenaria* neoplastic cells is much lower (1.2%) and is similar to that  
314 estimated in the heavily diseased mussels that we observed in the present work. Accordingly,  
315 we assumed that, above the threshold level of 5% of non-diploid nuclei, an ongoing neoplastic  
316 process occurs with a continuum of cellular modifications and an increase of the ploidy level

317 in which impaired mitosis plays an important role. Indeed, impaired mitosis has been shown  
318 to negatively affect genome stability by causing whole chromosome aneuploidy and also by  
319 promoting the acquisition of potentially tumor-promoting mutations (Ganem and Pellman  
320 2012). Thus, aneuploidies affecting the whole chromosome or only a segment of the  
321 chromosome can alter gene copy number of relevant oncogenes and tumor suppressors, at  
322 least in part by facilitating loss of heterozygosity of known tumor suppressor genes (Weaver  
323 et al., 2007; Baker et al., 2009). A number of cellular defects are known to generate whole  
324 chromosome aneuploidy, including atypical mitotic spindle assembly, inefficient chromosome  
325 distribution, abnormal microtubule dynamics, supernumerary centrosomes, and a defective  
326 spindle assembly checkpoint (Compton, 2011; Gordon et al., 2012; Holland and Cleveland,  
327 2012). All these cellular defects manifest during mitosis when chromosomes physically  
328 separate. Thus, it is widely accepted that abnormal mitosis can contribute to tumorigenesis via  
329 the generation of aneuploidy.

330 In several areas of the world, disseminated neoplasia reaches epizootic prevalence in some  
331 bivalve species causing serious regional economic damage to the aquaculture industry  
332 (Ciocan and Sunila 2005). The high prevalence of mussels affected by high prevalence of  
333 genetic abnormalities in relation to an ongoing neoplastic process (this work) and previous  
334 association of the same genetic abnormalities with mortality outbreaks in France  
335 (Benabdelmouna and Ledu 2016), indicate that this disease could be considered an important  
336 morbidity and mortality cause for mussels cultured in France. The techniques used in this  
337 work, and most principally FCM, could be powerful tools to help manage current mussel  
338 mortality, allowing determination of cytogenetic quality of wild and cultivated mussel beds  
339 with the aim of preserving good quality animals and eliminating/reducing individuals of poor  
340 quality, and the use of FCM-qualified juveniles as seeds in cultured stocks.

341

342 **Acknowledgements:**

343 The authors are grateful to J. Normand for help in mussel stock sampling and to the LGPMM  
344 hatchery staff for technical assistance in the hatchery. We also thank JF Pepin for critical  
345 reading of the manuscript. This work was funded by the French DPMA (Direction des  
346 pêchesmaritimeset de l'aquaculture, DPMA-2017-MORBLEU CONVENTION N°:  
347 17/1212952).

348

349 References

- 350 Baker, D.J., Jin, F., Jeganathan, K.B., van Deursen. J.M., 2009. Whole chromosome  
351 instability caused by Bub1 insufficiency drives tumorigenesis through tumor suppressor  
352 gene loss of heterozygosity. *Cancer Cell*. 16, 475–486.
- 353 Barber, B.J., 2004. Neoplastic diseases of commercially important marine bivalves. *Aquat.*  
354 *Living. Resour.* 17, 449–466.
- 355 Béchemin, C., Soletchnik, P., Polsenaere, P., Le Moine, O., Pernet, F., Protat, M., Fuhrman,  
356 M., Quéré, C., Goulitquer, S., Corporeau, C., Lapègue, S., Travers, A., Morga, B.,  
357 Garrigues, M., Garcia, C., Haffner, P., Dubreuil, C., Faury, N., Baillon, L., Baud, J-P.,  
358 Renault. T., 2015. Episodes de mortalité massive de moules bleues observés en 2014  
359 dans les Pertuis charentais. *Bulletin épidémiologique, santé animale et alimentation*,  
360 67, 6-9.
- 361 Benabdelmouna, A., Ledu, C., 2016. The mass mortality of blue mussels (*Mytilus spp.*) from  
362 the Atlantic coast of France is associated with heavy genomic abnormalities as  
363 evidenced by flow cytometry. *J. Invertebr. Pathol.* 138, 30-38.
- 364 Bihari, N., Micic, M., Batel, R., Zahn, R.K., 2003. Flow cytometric detection of DNA cell  
365 cycle alterations in hemocytes of mussels (*Mytilus galloprovincialis*) off the Adriatic  
366 coast. Croatia. *Aquat. Toxicol.* 64, 121–129.
- 367 Bower, S., 1989. The summer mortality syndrome and haemic neoplasia in the blue mussels  
368 (*Mytilus edulis*) from British Columbia. *Can. Tech. Rep. Fisheries Aquat. Sci.* 1703, 1–  
369 65.
- 370 Carballal, M.J., Barber, B.J., Iglesias, D., Villalba, A., 2015. Neoplastic diseases of marine  
371 bivalves. *J. Invertebr. Pathol.* 131, 83-106.

372 Carella, F., De Vico, G., Landini, G., 2017. Nuclear morphometry and ploidy of normal and  
373 neoplastic haemocytes in mussels. Plos One. 12 (3), e0173219.

374 Carella, F., Figueras, A., Novoa, B., De Vico, G., 2013. Cytomorphology and PCNA  
375 expression pattern in bivalves *Mytilus galloprovincialis* and *Cerastoderma edule* with  
376 haemic neoplasia. Dis. Aquat. Org. 105, 81-87.

377 Ciocan, C., Sunila, I., 2005. Disseminated neoplasia in blue mussels, *Mytilus*  
378 *galloprovincialis*, from the Black Sea, Romania. Mar. Pollut. Bull. 50, 1335-1339.

379 Collins, C., 1998. Studies on a Neoplasm of the Cockle, *Cerastoderma edule* (Linnaeus). Ph.  
380 D. Thesis Dissertation, National University of Ireland, Cork, pp. 155.

381 Compton, D.A. 2011. Mechanisms of aneuploidy. Curr. Opin. Cell Biol. 23, 109–113.

382 da Silva, P.M., Soudant, P., Carballal, M.J., Lambert, C., Villalba, A., 2005. Flow cytometric  
383 DNA content analysis of neoplastic cells in haemolymph of the cockle *Cerastoderma*  
384 *edule*. Dis. Aquat. Organ. 67, 133–139.

385 Delaporte, M., Synard, S., Pariseau, J., McKenna, P., Tremblay, R., Davidson, J., Berthe, F.C,  
386 2008. Assessment of haemic neoplasia in different soft shell clam *Mya arenaria*  
387 populations from eastern Canada by flow cytometry. J. Invert. Pathol. 98,190-197.

388 Diaz, S., Villalba, A., Insua, A., Soudant, P., Fernandez-Tajes, J., Mendez, J., Carballal, M.J.,  
389 2011. Disseminated neoplasia causes changes in ploidy and apoptosis frequency in  
390 cockles *Cerastoderma edule*. J. Invertebr. Pathol. 113, 214–219.

391 Dixon, D.R., Jones, I.M., Harrison, F.L., 1985. Cytogenic evidence of inducible processes  
392 linked with metabolism of a xenobiotic chemical in adult and larval *Mytilus edulis*. Sci  
393 Total Environ. 46, 1-8.

394 Elston, R.A., Drum, A.S., Allen, S.K., 1990. Progressive development of circulating  
395 polyploid cells in *Mytilus* with hemic neoplasia. Dis. Aquat. Organ. 8, 51–59.

396 Elston, R.A., Kent, M.L., Drum, A.S., 1988. Progression, lethality and remission of hemic  
397 neoplasia in the bay mussel, *Mytilus edulis*. Dis. Aquat. Org. 4, 135–142.

398 Elston, R.A., Moore, J.D., Brooks, K., 1992. Disseminated neoplasia of bivalve molluscs.  
399 Rev. Aquat. Sci. 6, 405-466.

400 FAO, 2014. Fisheries and aquaculture software. FishStatJ - software for fishery statistical time  
401 series. FAO Fisheries and Aquaculture Department Rome.  
402 <http://www.fao.org/fishery/statistics/software/fishstatj/en>.

403 Farley, C.A., 1969. Sarcomatid proliferative disease in a wild population of blue mussels  
404 (*Mytilus edulis*). J. Natl. Cancer Inst. 43 (2), 509–516.

405 Farley, C.A., Otto, S.V., Reinisch, C.L., 1986. New occurrence of epizootic sarcoma in  
406 Chesapeake Bay soft shell clams, *Mya arenaria*. Fish. B-NOAA 84, 851–857.

407 Fuentes, J., Lopez, J.L., Mosquera, E., Vazques, J., Villalba, A., Alvarez, G., 2002. Growth,  
408 mortality, pathological conditions and protein expression of *Mytilus edulis* and *M.*  
409 *galloprovincialis* crosses cultured in the Ria de Arousa (NW Spain). Aquaculture 213,  
410 233–251.

411 Galimany, E., Sunila, I., 2008. Several cases of disseminated neoplasia in mussels *Mytilus*  
412 *edulis* (L.) in Western Long Island Sound. J. Shellfish Res. 27, 1201-1207.

413 Ganem, N.J., Pellman, D. 2012. Linking abnormal mitosis to the acquisition of DNA damage.  
414 J. Cell. Biol. 6, 871-881.

415 Gordon, D.J., Resio, B., Pellman, D., 2012. Causes and consequences of aneuploidy in  
416 cancer. Nat. Rev. Genet. 13, 189–203.

417 Le Grand, F., Kraffe, E., de Montaudouin, X., Villalba, A., Marty, Y., Soudant, P., 2010.  
418 Prevalence, intensity, and aneuploidy patterns of disseminated neoplasia in cockles

419           (*Cerastoderma edule*) from Arcachon bay: seasonal variation and position in sediment.  
420           J. Invertebr. Pathol. 104, 110–118.

421   Lowe, D.M., Moore, M.N., 1978. Cytology and quantitative cytochemistry of a proliferative  
422           atypical haemocytic condition in *Mytilus edulis*. J. Natl. Cancer Inst. 60, 1455-1459.

423   Moore, J.D., Elston, R.A., Drum, A.S., Wilkinson, M.T., 1991. Alternate pathogenesis of  
424           systemic neoplasia in bivalve mollusk *Mytilus*. J. Invert. Pathol. 58, 231-243.

425   Myrand, B., Guderley, H., Himmelman, J., 2000. Reproduction and summer mortality of blue  
426           mussels *Mytilus edulis* in the Magdalen Islands, southern Gulf of St. Lawrence. Mar.  
427           Ecol. Prog. Ser. 197, 193–207.

428   Reno, P.W., House, M., Illingworth, E., 1994. Flow cytometric and chromosome analysis of  
429           soft-shell clams *Mya arenaria* with disseminated neoplasia. J. Invertebr. Pathol. 64 (2),  
430           163–172.

431   RStudio Team (2015). RStudio: Integrated Development for R. RStudio, Inc., Boston, MA  
432           URL <http://www.rstudio.com/>.

433   Sequim, W.A., Holland, A.J., Cleveland, D.W., 2012. Losing balance: the origin and impact  
434           of aneuploidy in cancer. EMBO Rep. 13, 501–514.

435   Smolarz, K., Thiriot-Quievreux, C., Wolowicz, M., 2005. Recent trends in the prevalence of  
436           neoplasia in the Baltic clam *Macoma balthica* (L.) from the Gulf of Gdańsk (Baltic  
437           Sea). Oceanologia 47 (1), 61-74.

438   Sunila, I., 1991. Respiration of sarcoma cells from the soft-shell clam *Mya arenaria* L. under  
439           various conditions. J. Exp. Mar. Biol. Ecol. 150 (1), 19–29.

440   Tremblay, R., Myrand, B., Sevigny, J.M., Guderley, H., 1998. Bioenergetic and genetic  
441           parameters in relation to susceptibility of blue mussels, *Mytilus edulis* (L.) to summer  
442           mortality. J. Exp. Mar. Biol. Ecol. 221, 27–58.

443 Usheva, L.N., Frolova, L.T., 2000. Neoplasia in the connective tissue of the mussel *Mytilus*  
444 *trossulus* from polluted areas of Nakhodka Bay in the Sea of Japan. Russ. J. Dev. Biol.  
445 31 (1), 63–70.

446 Vassilenko, E., Baldwin, S. A., 2014. Using flow cytometry to detect haemic neoplasia in  
447 mussels (*Mytilus trossulus*) from the Pacific Coast of Southern British Columbia,  
448 Canada. J. Invert. Pathol. 117, 68-72.

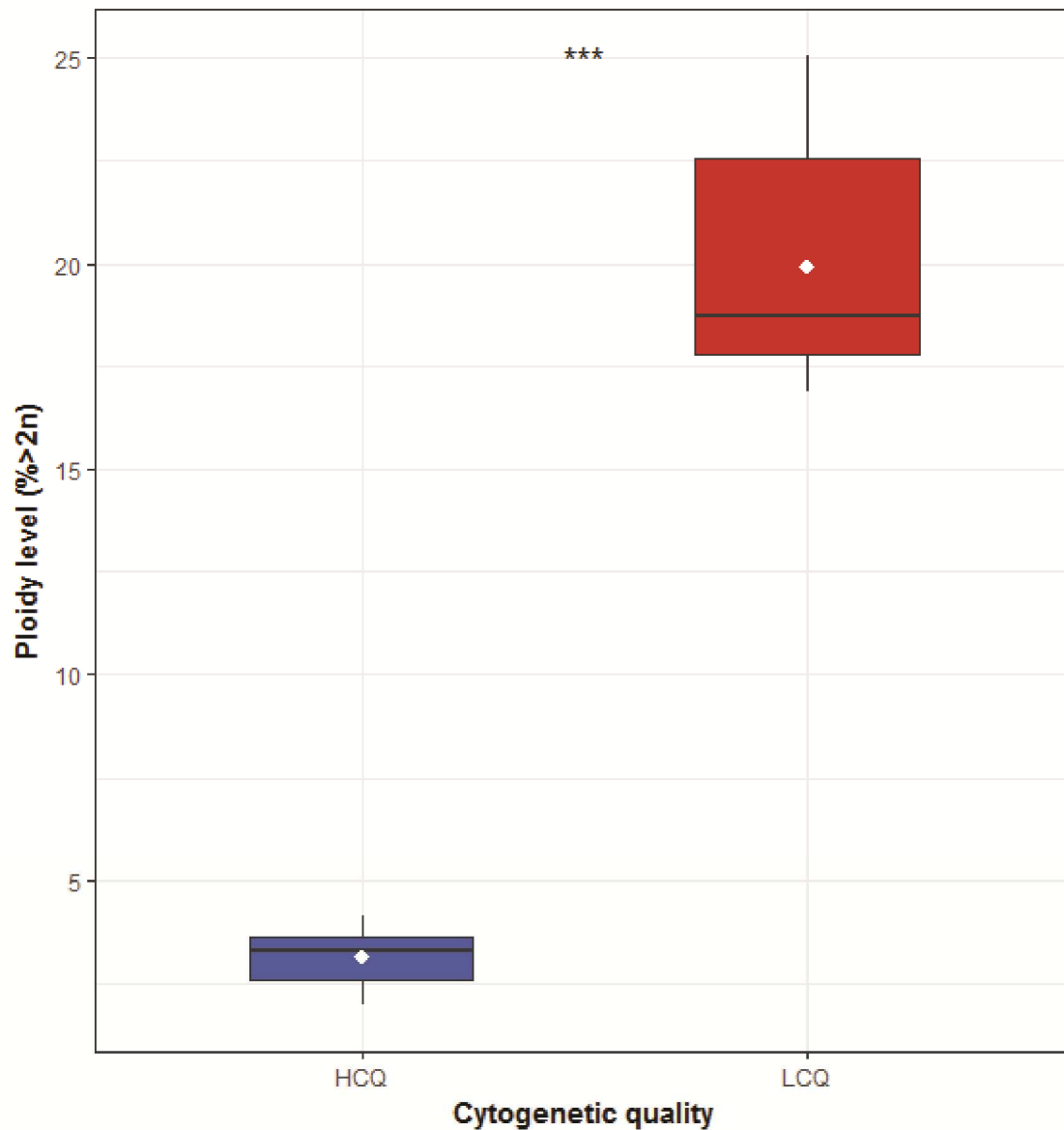
449 Villalba, A., Carballal, M.J., Lopez, C., 2001. Disseminated neoplasia and large foci  
450 indicating heavy haemocytic infiltration in cockles *Cerastoderma edule* from Galicia  
451 (NW Spain). Dis. Aquat. Organ. 46, 213–216.

452 Villalba, A., Peters, E.C., Lopez, M.C., Caraballal, M.J., 1995. Disseminated sarcoma in the  
453 clam *Ruditapes decussatus* in Galicia (NW Spain). J. Invert. Pathol. 65, 76-78.

454 Weaver, B.A.A., Silk, A.D., Montagna, C., Verdier-Pinard, P., Cleveland.D.W., 2007.  
455 Aneuploidy acts both oncogenically and as a tumor suppressor. Cancer Cell. 11, 25–36.

456 Wickham, H., 2009. ggplot2: Elegant Graphics for Data Analysis. Springer-Verlag New  
457 York.

458



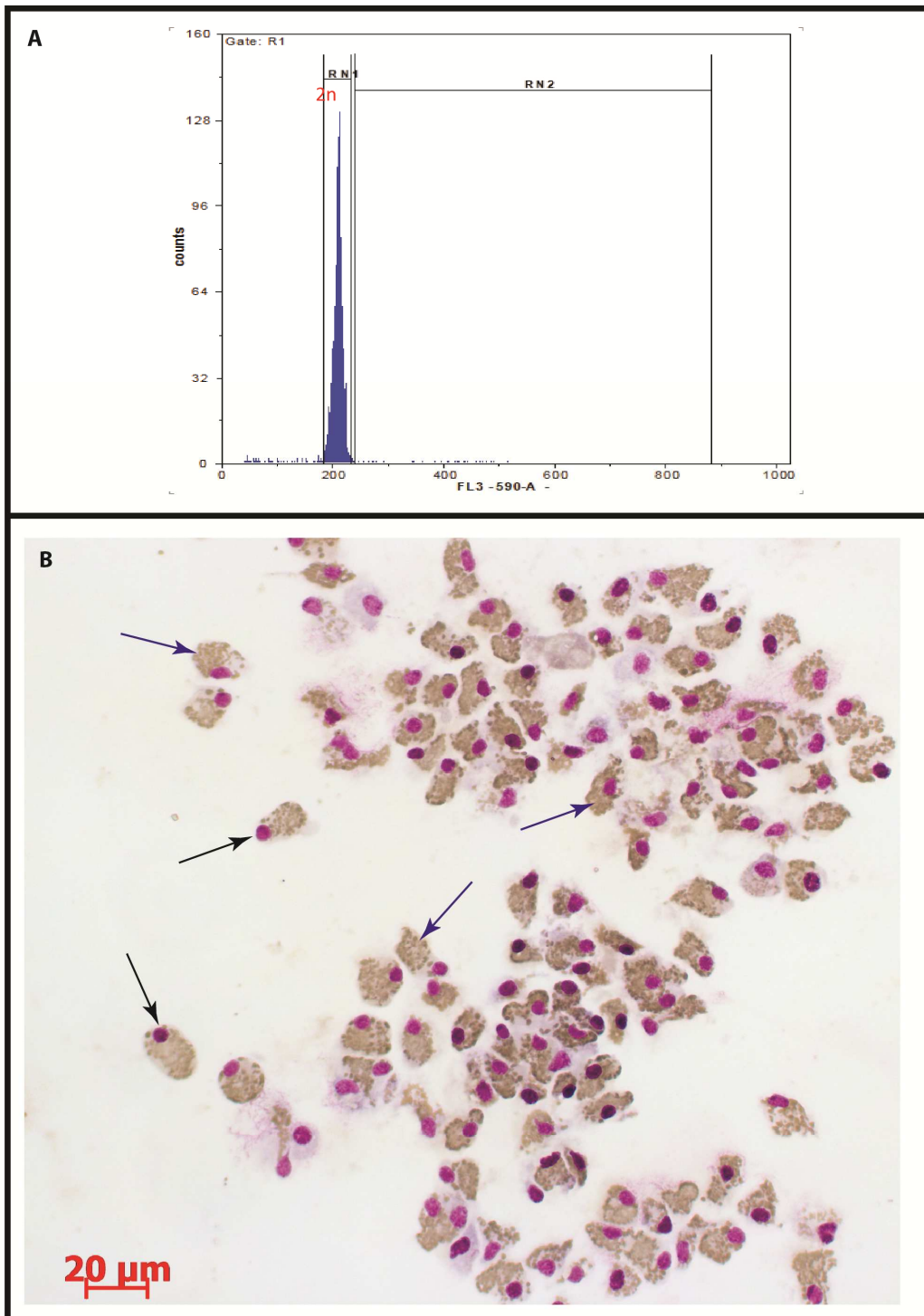
459

460

461 **Figure 1: Variation of the non-diploid nuclei percentages within and between the two**  
 462 **mussel stocks according to cytogenetic quality.**

463 HCQ: High Cytogenetic Quality (blue boxplot), LCQ: Low Cytogenetic Quality (red  
 464 boxplot). The upper, central and lower horizontal bars of the boxes indicate the 3rd quartile,  
 465 median and 1st quartile, respectively. Upper and lower extremities of the whiskers represent  
 466 the minimum and maximum values for each variable. Filled white diamonds correspond to  
 467 mean values. Asterisks display significant differences between HCQ and LCQ ('\*\*\*'  $p <$   
 468  $0.001$  after tests of Wilcoxon).

469



470

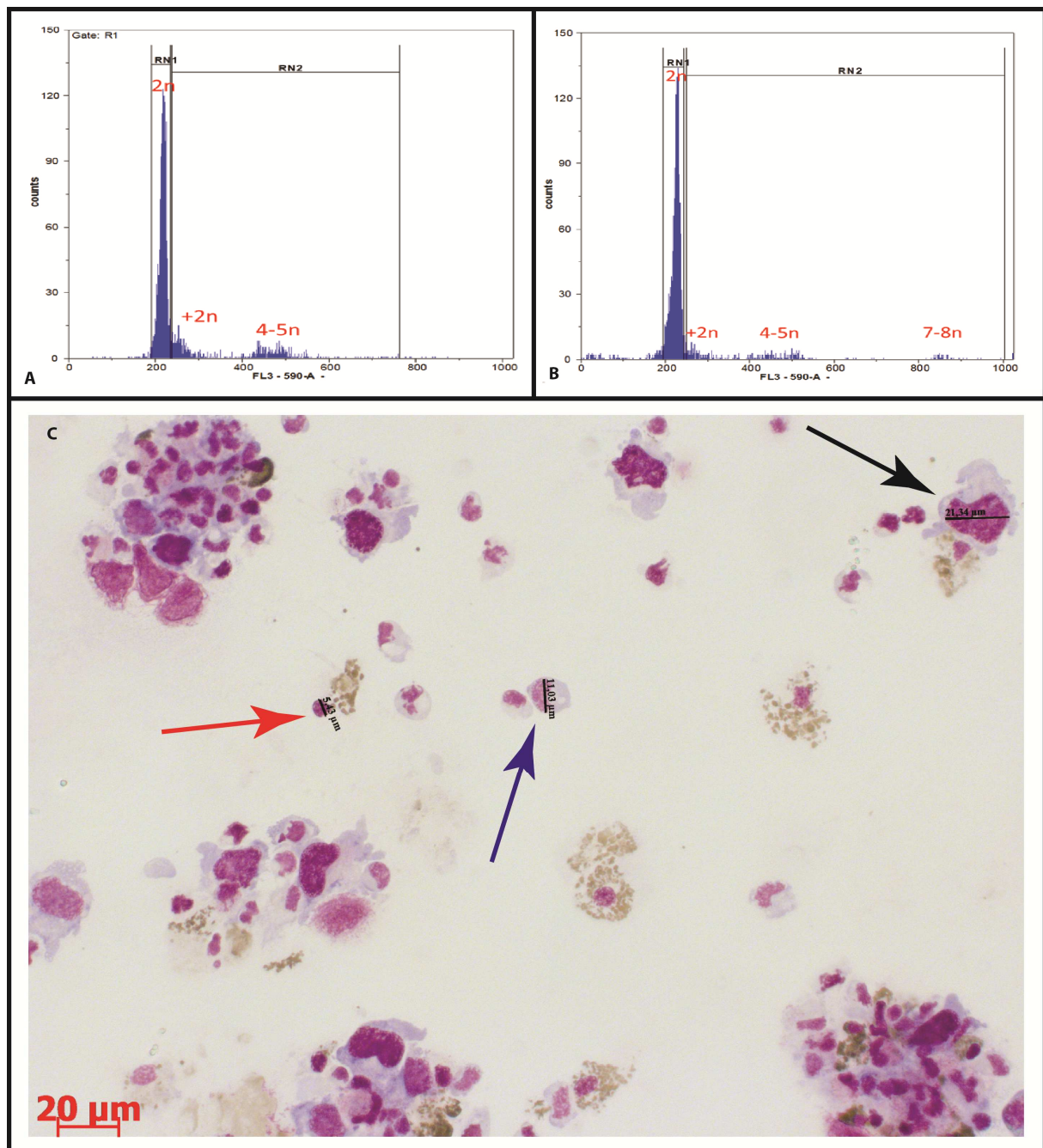
471

472 **Figure 2: Flow cytometry and hemocytology analysis of HCQ blue mussels.**

473 (A) Flow cytometry histogram of propidium iodide stained hemolymph nuclei from normal  
 474 HCQ blue mussels. Histogram of propidium iodide fluorescence of gated single nuclei show  
 475 Markers RN1 and RN2 placed to estimate the percentage of nuclei in diploid (2n) and non-  
 476 diploid phases, respectively. (B) Hemolymph cell-monolayer preparation showing a large  
 477 majority of normal granulocytes with nucleus stained dark purple (black arrows) and  
 478 cytoplasm light purple (blue arrows).

479

480



481

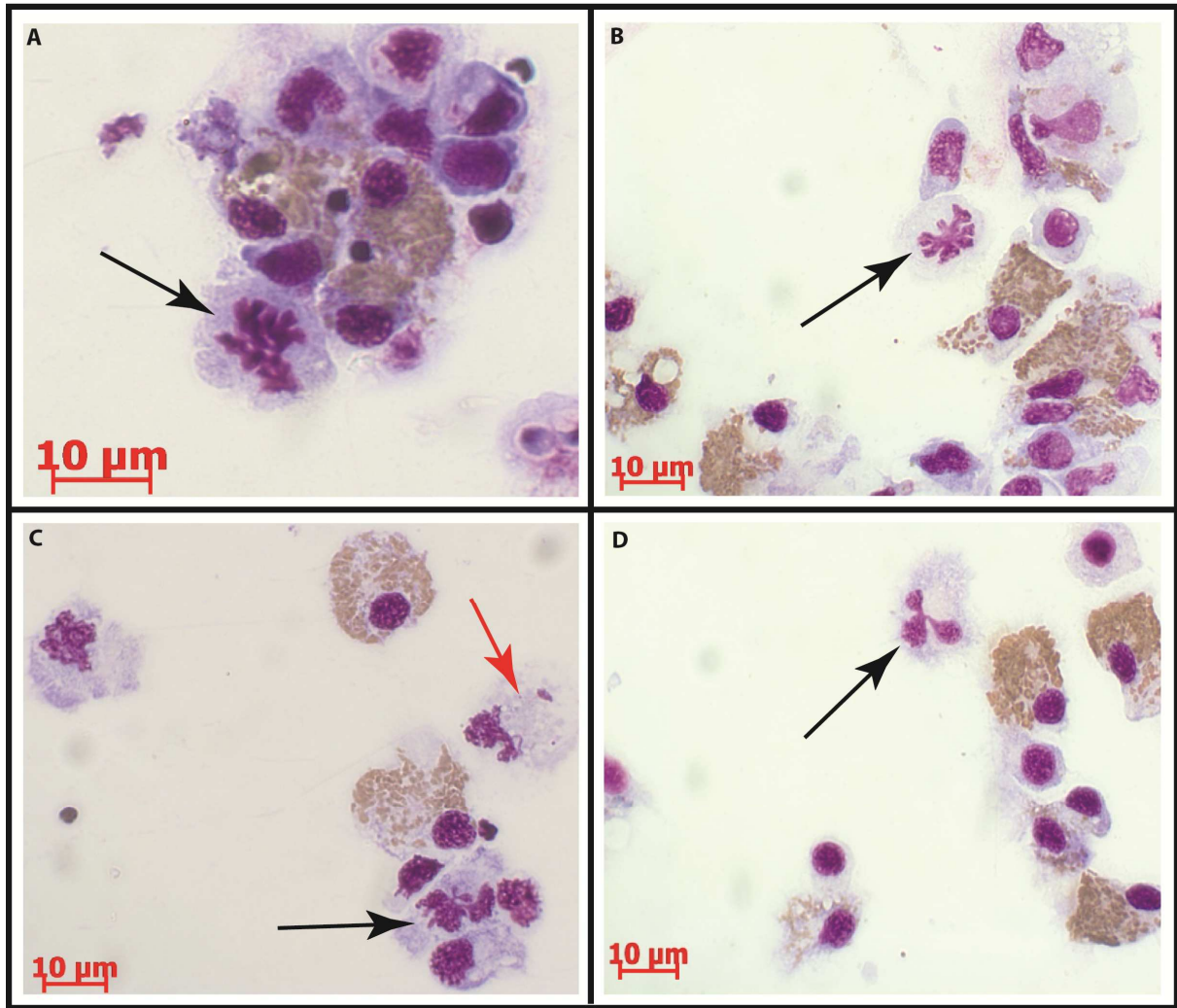
482

483 **Figure 3: Flow cytometry and hemocytology analysis of LCQ blue mussel.**

484 (A) and (B) Flow cytometry histograms of propidium iodide stained hemolymph nuclei from  
 485 abnormal blue mussels. Histogram of propidium iodide fluorescence of gated single nuclei  
 486 with markers RN1 and RN2 placed to estimate the percentage of nuclei in diploid (2n) and  
 487 non-diploid phases. (A-B), Non-diploid nuclei included hyperdiploid-hypotriploid (2-3 n) to  
 488 tetraploid-pentaploid (4-5 n) nuclei and (B) heptaploid-octoploid nuclei (7-8 n). (C)  
 489 hemolymph cell-monolayer preparation showing few normal granulocytes with nucleus of  
 490 normal mean size (5-6 μm of diameter, red arrow) and a majority of abnormal neoplastic cells  
 491 that are rounded in shape with a reduced, granulation-free cytoplasm enclosing large (11-12  
 492 μm, blue arrow) to very large nuclei (up to 20 μm, black arrow).

493

494



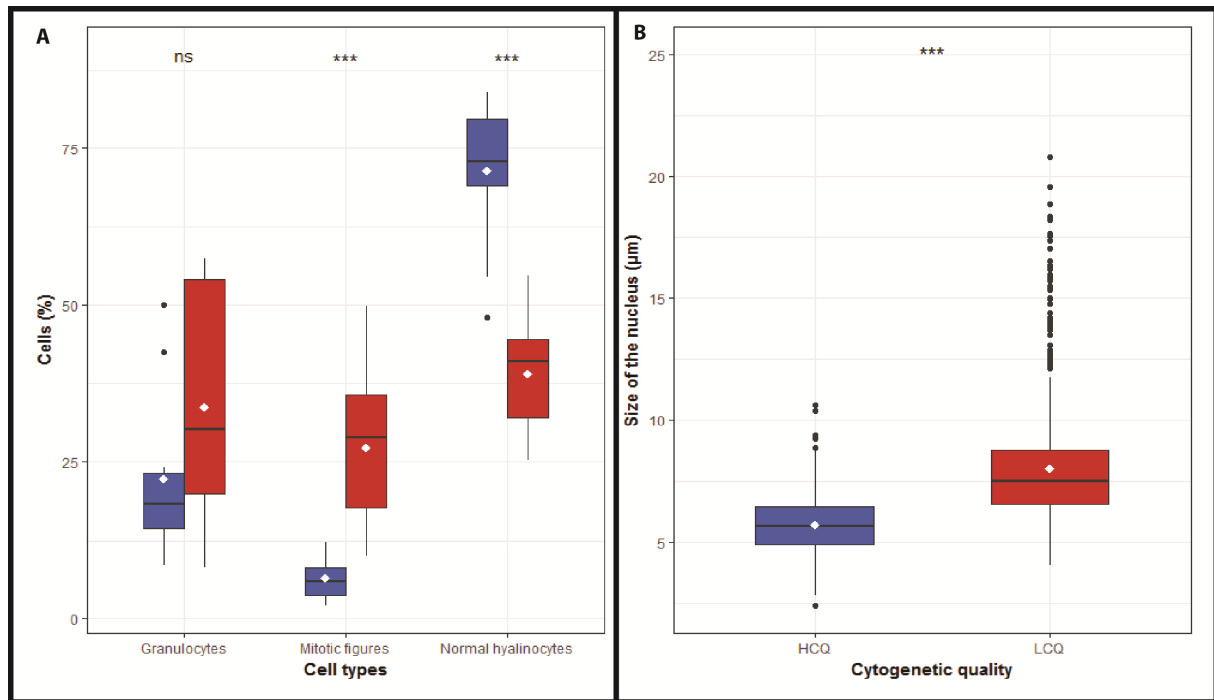
495

496

497 **Figure 4: Hemocytology analysis of LCQ mussels with abnormal mitotic figures.**

498 Black arrows indicate mitotic figures with abnormal segregation pattern including, star-like  
499 (B), unequal (A, C) and tripolar (D) segregation. (C) Red arrow indicates an unequal  
500 segregation pattern with lagging chromosomes.

501



502

503

504 **Figure 5: Analysis of cell characteristics from each mussel group LCQ and HCQ.**

505 (A) Number of cells by cell types and (B) Nuclei sizes for HCQ and LCQ quality. HCQ: High  
 506 Cytogenetic Quality (blue boxplot), LCQ: Low Cytogenetic Quality (red boxplot). The upper,  
 507 central and lower horizontal bars of the boxes indicate the 3rd quartile, median and 1st  
 508 quartile, respectively. Upper and lower extremities of the whiskers represent the minimum  
 509 and maximum values for each variable. Filled white diamonds correspond to mean values.  
 510 Asterisks display significant differences between HCQ ('\*\*\*'  $p < 0.001$  after tests of  
 511 Wilcoxon) vs LCQ ('ns': non significance,  $p > 0.05$ ).